Proceedings World Geothermal Congress 2020+1
Reykjavik, Iceland, April - October 2021

Stress Preconditioning for Critically-Stressed EGS Reservoir Stimulation in Reverse Faulting Stress Regimes

Barnaby Fryer[1], Xiaodong Ma[2,3], Gunter Siddiqi[4], and Lyesse Laloui[1]

[1]Laboratory for Soil Mechanics, Ecole Polytechnique Fédérale de Lausanne, Station 18, 1015 Lausanne, Switzerland

[2]Swiss Competence Center for Energy Research – Supply of Electricity (SCCER-SoE)

[3]Chair for Geothermal Energy and Geofluids, ETH Zürich, Zürich, Switzerland

[4]Swiss Federal Office of Energy, Bern, Switzerland

barnaby.fryer@epfl.ch

Keywords: Hydraulic stimulation, reservoir engineering, poroelastic stresses

ABSTRACT

Using numerical simulations, it is suggested that it is possible to direct stimulation treatments in EGS wells away from previously stimulated wells in critically-stressed reverse faulting stress regimes. This is done by producing fluid out of the previously stimulated zones associated with other wells in a preconditioning phase. Then, the poroelastic stress changes, and not the pore pressure decreases, associated with this production phase repel the stimulation treatment of the new well. This occurs because production induces horizontal total stress decreases in areas at the same depth as the producing zone. In a reverse faulting stress regime, the maximum principal stress is horizontal and these horizontal stress reductions act to inhibit shear failure and therefore stimulation. This work implies that reservoir engineers may have some control in designing their stimulation treatments in large geothermal fields and may be of use in avoiding potential seismic faults and creating flow paths which are long enough to sufficiently heat a cycling fluid.

1. INTRODUCTION

Generally, Enhanced Geothermal Systems (EGS's) require the creation of high permeability pathways to establish inter-well connectivity and fluid circulation. The creation of these permeable pathways is critical for the successful commercial development of EGS in a power generation context (Robinson et al., 1971; Ziagos et al., 2013). Therefore, technologies or methodologies which are able to help guide the direction in which reservoir stimulation occurs would represent a significant step forward for the EGS industry. While the ability to draw a stimulation treatment towards another well would have obvious advantages in terms of creating inter-well connectivity, the ability to repel a stimulation treatment may also be useful. Specifically, the ability to repel a stimulation treatment may allow engineers to more easily avoid stimulating near a large fault or it may help in the creation of long fluid pathways, reducing the chance short-circuiting.

The criticality of the stress field is a crucial parameter for a stimulation procedure. Reservoirs with a higher stress criticality are more readily stimulated than those with a low stress criticality. For this reason, an attempt will be made here to guide a stimulation treatment by altering the stress criticality of the reservoir near the well. Previously, production (e.g., Segall, 1989), injection (e.g., Chen et al., 2017), and hydraulic fracturing (e.g., Deng et al., 2016) induced seismicity has made it clear that reservoir engineering operations are capable of altering the stress field even without local pore pressure changes. Production will therefore be used here to alter the stress field before stimulation. Of course, EGS reservoirs are usually quite impermeable initially. For this reason, production will take place from an adjacent well located in a previously stimulated section of reservoir.

The possibility of directing reservoir stimulation treatments has been investigated previously. In the oil and gas industry, this was initially focused on altering the stress field in order to influence the orientation of an eventual hydraulic fracture (Shuck, 1977; Warpinski and Branagan, 1989). Other investigations included such topics as the possibility of altering the stress state such that a hydraulic fracture would be more likely to connect two wells have also been investigated (Boutéca et al., 1983). These investigations have not been limited to the oil and gas industry, however, with Baria et al. (2004) showing the positive influence contemporaneous stimulation could have on two wells' inter-connectivity in the context of an EGS project in crystalline rock. This study was primarily focused on the influence of the elevated pore pressure resulting from joint stimulation, however.

EGS reservoirs are typically thought to be stimulated in shear, especially when the injection pressure is below the minimum principal stress (e.g., Zang et al., 2014), although there are reports of mixed-mode in certain cases (e.g., McClure and Horne 2014). Shear failure is controlled by Coulomb faulting theory in the case of pre-existing planes of weakness, with such planes being typical in EGS reservoirs. Coulomb faulting theory implies that increases in pore pressure will bring a potential shear plane closer to failure, with both the maximum and minimum principal stresses decreasing by an equivalent amount. Generally, this is thought to be the primary mechanism inducing shear failure in EGS reservoirs (e.g., Pearson 1981). This shear failure can be induced at pore pressures below the minimum principal stress fundamentally separating it from hydraulic fracturing. Changes to total stress can also lead to shear failure, however. The isotropic reduction of both the maximum and minimum principal stresses can lead to shear failure in much the same way as pore pressure increases; however, in certain instances the total stresses may change anisotropically. This has been seen, for example, in production-induced seismicity (e.g., Segall 1989). It could be argued that changes to total stress, through poroelasticity for example, are in some ways more effective at inducing shear failure than pore pressure increases because it is not only possible to lower the effective stresses, it is also possible to increase the differential stress through anisotropy. In most cases, however, the changes to total stress are much smaller than those to pore pressure, leading to many cases of pore pressure change being the dominant mechanism leading to shear failure. That said, total stress changes can be large enough to have a significant effect in certain cases. Here, the influence of total stress changes due to poroelasticity will be the subject of investigation.

The focus here will concern three horizontal wells drilled into crystalline rocks, in this case a granite in a critically-stressed reverse faulting stress regime. The wells will be drilled horizontally, as it is becoming increasingly common to see directional EGS wells (e.g., Kwiatek et al., 2019). The wells will be drilled to the same depth in the direction of the minimum principal stress. Initially, the one of the wells will be stimulated following a procedure similar to those seen in the industry. This stimulation treatment will connect to a second well, creating a doublet system. These two wells will then be produced. This marks the preconditioning phase of the methodology. A third well, outside of the previously stimulated zone will then be stimulated. The analysis will concern the effect of the preconditioning phase on the stimulation treatment of the third well, with the goal of repelling the stimulation treatment of the third well away from the first two wells. Specifically, an attempt will be made to direct the stimulation treatment using primarily the poroelastic stress changes that occur during production, not the pore pressure decrease.

2. PROBLEM SETUP

The 2-D model domain (Figure 1) will be limited to a section of the crystalline reservoir, extending over a lateral domain of 10 km and a vertical domain of 4000 m. The depth of the wells will be set at 4500 m, a reasonable depth for EGS wells. The overburden which is not contained in the model (up to 2500 m) will be replaced by a constant stress based on a reasonable lithostatic gradient. A reverse faulting stress regime will be assumed and the wells will be horizontal, drilled parallel to the minimum horizontal stress, S_{hmin} which is normal to the plane of the model. The initial vertical stress and pore pressure in the model will be calculated using lithostatic and hydrostatic gradients, respectively. The maximum horizontal stress, S_{Hmax}, is then found by assuming that the crust is critically-stressed (e.g., Brudy et al., 1997). This is done by assuming that the reservoir is in frictional equilibrium, using a coefficient of friction of 0.6.

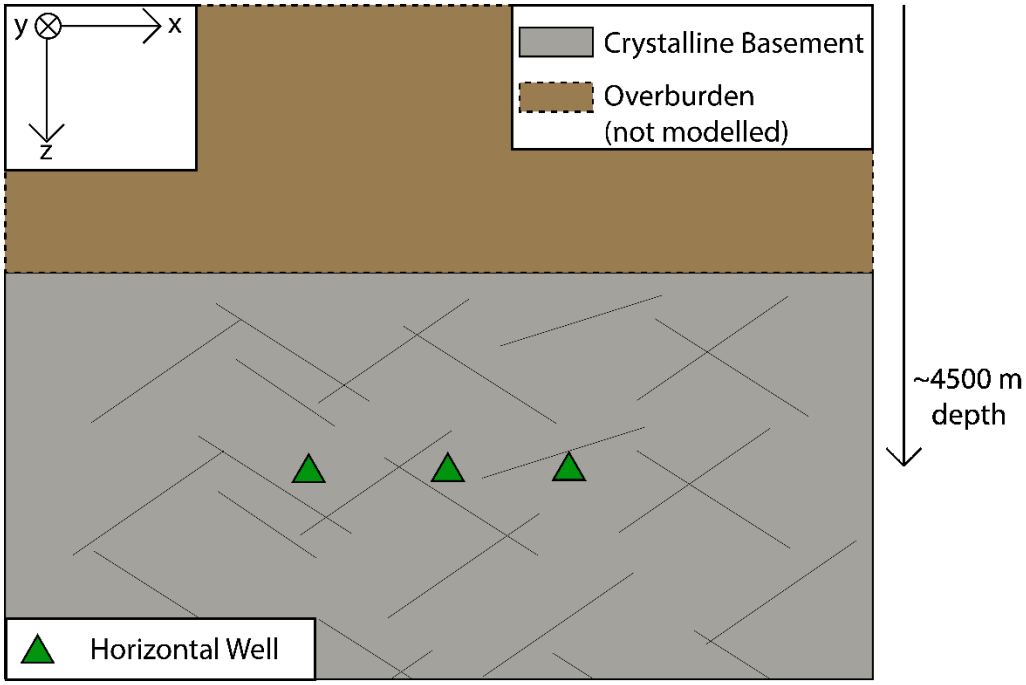

Figure 1: The problem setup. Note that the figure is not to scale. The horizontal wells are separated by 1079m horizontally and are located at the same depth.

The intact Young's modulus will be taken as 36 MPa (Villeneuve et al., 2018); however, the rock is assumed to be fractured, which can be assumed to lower Young's modulus for the bulk (e.g., Pimienta et al., 2019). A bulk Young's modulus of 50 % of the intact Young's modulus was used following findings of Villeneuve et al., 2018. As fractures are not explicitly modelled in this approach, it is this bulk Young's modulus which is ultimately input into the model. For the Biot coefficient, a value of 0.76 is used. This value is high for a granite, but is reasonable for highly fractured rock and has been previously been seen in the field (Evans et al., 2003). Poisson's ratio is taken as 0.15, a low value for granite which results from its fractured nature in this case (Walsh, 1965). Finally, porosity will be taken as 0.02, with the in-situ fractures acting as the only fluid conduits.

The three horizontal wells present in the model are all located at the same depth and are separated by 1079 m. The left-most well is stimulated first with an injection rate of 0.0254 kg/sec m over the course of 4 days, resulting in a total injection of 4.4e6 kg over this length of well (500 m), representing a small stimulation treatment. The stimulated zone resulting from this stimulation treatment reaches the center well. After this initial stimulation period, both the left-most and the center well are produced at a rate of 0.002 kg/sec m, resulting in 6.9e6 kg production from each well. This is the preconditioning stage of the operation. The production rate used in this stage is significantly lower than what are considered to be commercial production rates for EGS (Ziagos et al., 2013). This preconditioning stage lasts for 80 days in this example. Finally, the right-most well is stimulated with an injection rate of 0.006 kg/sec m for a period of three days. During this final stimulation, no production or injection occurs in the right-most or center wells.

To simplify the analysis, an isothermal simulation will be performed. While this is not a realistic scenario for stimulation in EGS reservoirs, it allows for the effects of the production-induced poroelastic stress preconditioning to be isolated and properly analyzed. The likely effects of the thermal strains are discussed in Section 5.

3. METHODOLOGY

Pressure and stress changes are modeled using a sequentially-coupled poroelastic simulator. The simulator employs the continuity equation for mass balance, the momentum balance equation, and the poroelastic version of Hooke's Law to compute these pressure and stress changes. The continuity equation for mass balance is used to model fluid flow, and the pore pressures resulting from this part of the model are used as inputs to solve for displacements and, ultimately, stresses in the mechanical model which is based on the momentum balance equation and Hooke's Law. The entire model is 2-D plane strain. Despite the 2-D setup, this type of model is appropriate to model 3-D stress changes resulting from reservoir engineering activities associated with a horizontal well (Cheng, 1998). Although this investigation involves reservoir stimulation, which by nature involves fractures and fissures, a dual-porosity model is not employed due to the assumed impermeability of the matrix. Instead, a bulk approach is used which takes averaged porosity and permeabilities appropriate for the size of the grid blocks present in the model.

3.1 Flow Model

The continuity equation for mass balance can be combined with Darcy's Law and written as,

$$\frac{\delta(\varphi\rho)}{\delta t} - \nabla \cdot \left(\frac{k}{\mu}\rho\big(\nabla P - \nabla(\rho g z)\big)\right) = q, \tag{1}$$

for a single phase. Here, φ is the porosity, ρ is the fluid density, k is the permeability, μ is the fluid's dynamic viscosity, P is the pore pressure, g the acceleration due to gravity, z the depth, and q the influx of mass. This equation is discretized in a finite volume in space, fully implicit finite difference in time framework (Aziz and Settari, 2002) and solved for one primary variable, pore pressure. All boundaries are no-flow boundaries except the top boundary which is a constant pressure boundary.

3.2 Mechanical Model

The mechanical model is developed beginning with the conservation of momentum,

$$\nabla \cdot \sigma' + \nabla(\alpha P) = -f, \tag{2}$$

where σ' represents the effective stress, α is the Biot coefficient, and f is the body forces. This equation is discretized in a finite element framework in combination with the linear theory of poroelasticity (Biot, 1941; Rice and Cleary, 1976; Wang, 2000),

$$S_{ij} - \alpha P \delta_{ij} = \frac{E}{(1+\nu)}\varepsilon_{ij} + \frac{E\nu}{(1+\nu)(1-2\nu)}\varepsilon_{kk}\delta_{ij}, \tag{3}$$

allowing for the model to solve for the stresses and strains associated with fluid production and injection. Here, S represents the total stress, δ_{ij} is the Kronecker delta, E is Young's Modulus, ν is Poisson's ratio, and ε_{ij} is the strain. Note that the use of pore pressure in the mechanical model represents the coupling from the flow model to the mechanical model. The coupling in the other direction is accomplished via permeability's dependence on stress, described in the following section. In the mechanical model all displacements perpendicular to the boundary are restricted except at the surface which is free.

3.3 Permeability

As mentioned, the permeability used in the model is based on a bulk approach. Typically, the type of rock targeted for EGS has a rather impermeable matrix and this is assumed to be the case for this model. Instead, the permeabilities of the grid blocks in the model will be assumed to be due to the potential for flow through faults and fractures present in the rock. These faults and fractures have a tendency to experience changes in aperture or even shear based on their orientation, their coefficients of friction, and the state of the stress. Based on this, the permeability in this model will change based on normal stress and increase in a stepwise fashion once a failure condition is reached (Miller, 2015). More specifically, based on Miller 2015's model, permeability will vary with normal stress as,

$$k = k_0 e^{\frac{-\bar{\sigma}}{\sigma*}}, \tag{4}$$

where the initial permeability is defined as k_0, $\bar{\sigma}$ is the effective normal stress on the potential shear plane, and σ* is a normalizing constant assumed to be equal to 100 MPa. At shear failure, which is defined based on Coulomb faulting theory, a stepwise change in permeability is assumed to occur, again following Miller 2015. In this case, k_0 in Equation 4 is replaced by k'_0, where k'_0 is defined as

$$k'_0 = x k_0. \tag{5}$$

Here, x is a factor which represents the increase in permeability associated with shear stimulation. This stepwise increase in permeability means that permeability increases associated with shear stimulation are assumed to remain after the stimulation treatment has been completed. A reasonable value for x can be chosen based on past shear stimulation treatments. For instance, at the Fjällbacka Hot Dry Rocks Projects, Sweden, permeability was seen to increase by three orders of magnitude following stimulation (Jupe et al., 1992). At Soultz, however, transmissivity only increased by a factor of fifteen (Evans et al., 2005a). Here, an increase of a factor of 200 will be taken, similar to the result of the shear stimulation treatment at Basel (Ladner and Häring, 2009).

Although the rocks generally associated with EGS require some form of stimulation before they are able to produce/inject fluid at economically-viable rates, these rocks are generally not impermeable in their initial state. Indeed, the permeability of the upper crust has been shown to be high ($10^{-17}\ m^2$ to $10^{-16}\ m^2$) due to shear failure on critically-stressed faults and fractures (Zoback and Townend, 2001). This notion is supported by pre-stimulation tests at both the Soultz HDR site and the Basel 1 enhanced geothermal

system which yielded effective permeabilities of $3 \cdot 10^{-16}\ m^2$ and $10^{-17}\ m^2$, respectively (Evans et al., 2005b; Häring et al., 2008; Ladner and Häring, 2009). For this reason, a value of $10^{-17}\ m^2$ is taken for k_0. Equations 4 and 5 represent the coupling from the mechanical model to the flow model.

3.4 Coulomb Stress

As mentioned, shear failure is assumed to occur based on Coulomb faulting theory. More specifically, Coulomb stress, defined as

$$\tau = \tau_s - \mu_f(S_n - P), \tag{6}$$

is used to determine whether or not shear failure has occurred. Here, τ_s is the shear stress, μ_f is the coefficient of friction, and S_n is the total normal stress on the assumed shear plane. Based on the findings of Evans et al., 2012, the reservoir will be assumed to be critically stressed here, and a Coulomb stress increase of 0.1 MPa will be considered sufficient to result in shear failure.

4. RESULTS

This section will evaluate three different stages of the proposed stimulation procedure which is designed to stimulate three equally-spaced wells with the goal of hydraulically connecting the first two wells and leaving the third well hydraulically isolated from the other two. First, the left-most of the three wells is stimulated. No special procedure is used here. As can be seen in Figure 2a, the injection of fluid associated with this injection causes large Coulomb stress increases near the well; this is due to an elevated pore pressure in this region. Further away from the well at the same depth the Coulomb stress still increases but not by as large an amount. This is due to the poroelastic stress changes associated with the injection. In this region, the horizontal total stresses increase. As this is a reverse faulting stress regime, an increase in horizontal total stress results in an increase in Coulomb stress. Above the well, Coulomb stress is decreased. This is due to the reduction in horizontal total stress and the increase in total vertical stress associated with the poroelastic stress changes due to injection.

The changes in Coulomb stress map to the increases in permeability seen in Figure 2b. Areas which have experienced large Coulomb stress increases are likely to experience shear stimulation. This leads to the stimulated zone primarily extending horizontally, with little vertical stimulation. In this case, the shear stimulation procedure was chosen such that the stimulated zone extends to the middle well and then stops. In reality it would be difficult to stimulate the reservoir this exactly. A more practical solution might be to stimulate the first well and then drill the second well into the stimulated zone as delineated by a microseismic cloud. The stimulated zone extends 1079m from the left-most well in both directions.

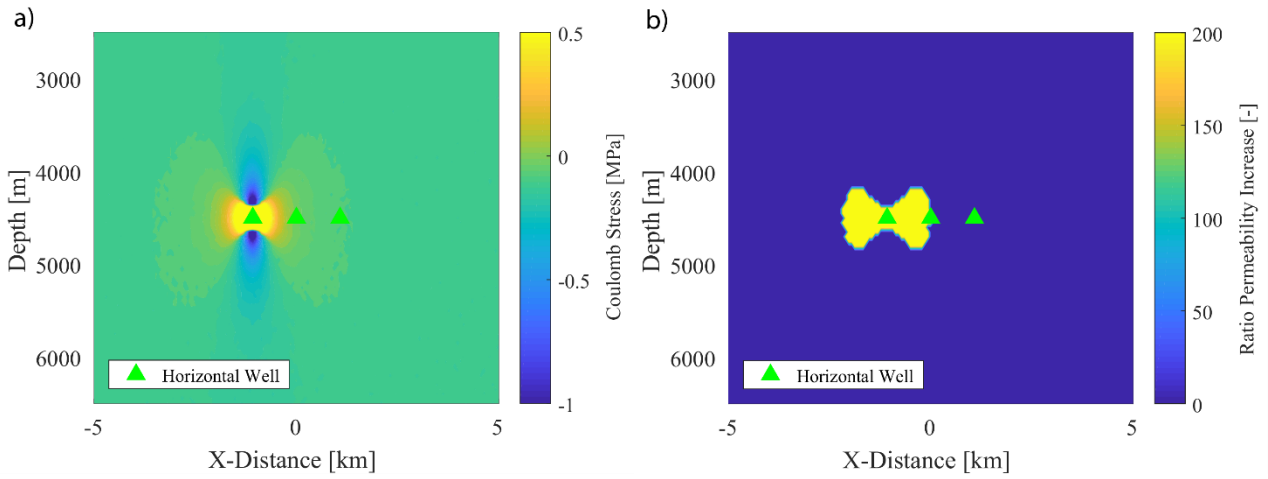

Figure 2: The (a) Coulomb stress changes and (b) region of permeability enhancement associated with the stimulation of the left-most well during phase 1. The stimulated region extends 1079m in either direction from the left-most well.

The second phase consists of producing both the left-most and middle wells. The reduced pore pressure results in a reduction in Coulomb stress near the wells, Figure 3a. Important to note is the reduction in Coulomb stress that this creates between the middle and right-most wells.

This production also results in an increase in Coulomb stress above and below the left-most and middle wells, however. This increase in Coulomb stress in these regions matches well with the Coulomb stress changes that lead to production-induced seismicity in reverse faulting stress regimes (Segall 1989). These Coulomb stress increases lead to shear failure and reservoir stimulation in these locations, Figure 3b.

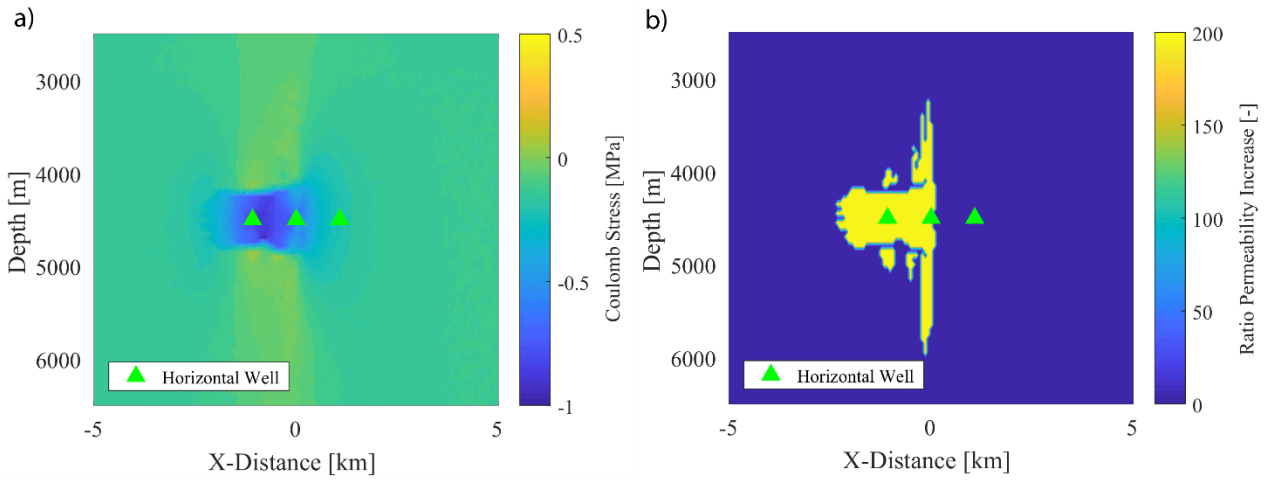

Figure 3: The (a) Coulomb stress changes and (b) region of permeability enhancement associated with the production from the left-most and middle wells during phase 2. The stress preconditioning associated with the production results in a zone of reduced Coulomb stress between the middle and right-most wells. Further, this production results in shear stimulation occurring above and below the two producing wells.

The third and final phase consists of the stimulation of the right-most well. As in the first phase, the injection associated with the stimulation treatment results in an increased pore pressure region near the well. This results in a region of Coulomb stress increase near the well, Figure 4a. To the right of the right-most well is another region of increased Coulomb stress, similar to that seen in Figure 2a. This region is again due to poreoelastic stress changes and is smaller in magnitude than the high pore pressure region near the wellbore. Above and below the wellbore show regions of reduced Coulomb stress due to poroelastic stress changes, again as in Figure 2a. The region between the middle and right-most wells also shows elevated Coulomb stress changes but these stress changes are smaller in magnitude than those to the right of the right-most well. This is a result of the stress preconditioning associated with the fluid production in phase 2.

The stimulation treatment in this third phase results in permeability enhancement around the right-most well, Figure 4b. The region between the middle and right-most wells remains largely unstimulated due to the Coulomb stress changes associated with the preconditioning phase described earlier. The permeability enhancement is able to extend to the right of the right-most well, however. Note that the stimulation treatment being directed is due to the poroelastic stress changes and not the reduced pore pressure near the middle well. For example, at a location 216m to the right of the middle well, the Coulomb stress change is -0.31 MPa but the decrease in pore pressure is only -0.06 MPa. This is due to the fact that it is difficult to reduce the pore pressure in the unstimulated regions, but the pore pressure decrease in the stimulated region is able to cause a poroelastic stress change in the unstimulated region. Ultimately, the stimulation treatment of the right-most well extends 1007m to the right and 576m to the left. This results in a gap between the stimulated zone of the right-most well and the middle well of 503m, leaving the two wells hydraulically isolated.

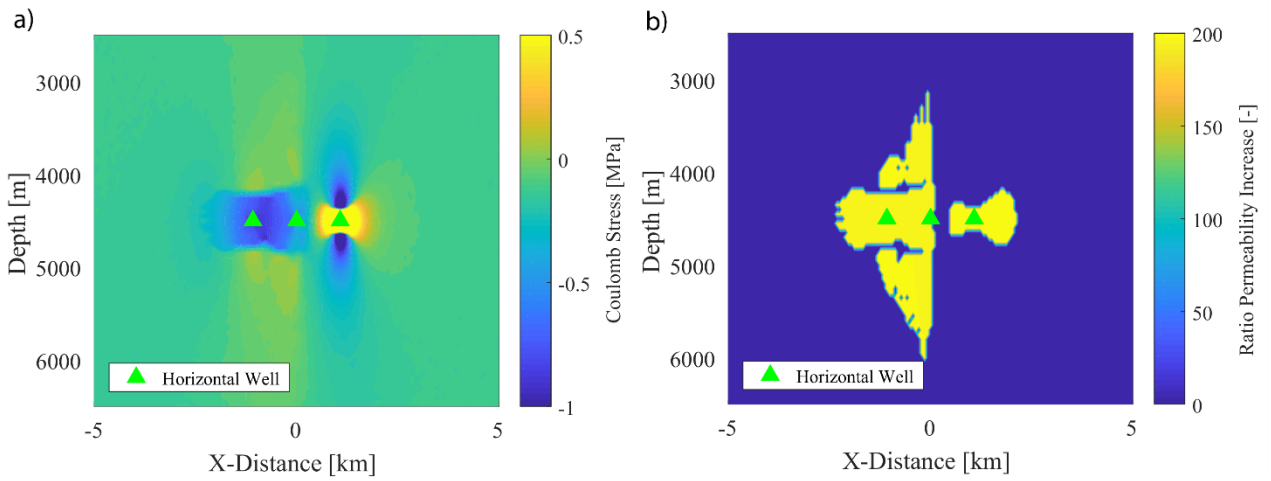

Figure 4: The (a) Coulomb stress changes and (b) region of permeability enhancement associated with the stimulation of the right-most well during phase 3. The stimulated region extends 576m to the left and 1007m to the right from the right-most well. There is an unstimulated gap of 503m between the middle well and the stimulated region of the right-most well.

5. DISCUSSION

5.1 Assumptions

In this analysis, it was assumed that the reservoir was critically stressed. Although this has generally been seen to be the case in EGS reservoirs in crystalline rock (Evans et al., 2012), it is possible that some reservoirs will either not be critically stressed or less critically stressed than the example case evaluated here. Indeed, in this case it was assumed that a Coulomb stress change of 0.1 MPa would be enough to incite shear failure. This value of Coulomb stress change is generally thought to be sufficient in the case that the crust is critically stressed (Stein, 1999). In the case that the crust is less critically stressed, however, the stimulated zones would have a different shape. More specifically, the zone of stimulation would correspond more closely to the zone of high pore pressure. This implies that the wings that developed on the outskirts of each stimulated zone would be restricted with the stimulated zone developing in a more circular pattern. Further, it would become more difficult to guide the stimulation treatment through stress preconditioning. This is because it is difficult to induce very large poroelastic stress changes to precondition the stress field of the reservoir, and, if the reservoir is less critically stressed, these poroelastic stress changes will have relatively less significance compared to the Coulomb stress change required to induce shear failure.

Stress redistribution due to shear failure is not considered in this model. It has been previously shown, however, that stress redistribution during stimulation can significantly influence the stress field, potentially having an impact on future slip events (e.g., Catalli et al., 2013). Certainly, stimulation treatments in granite have been seen to alter the stress field through aseismic slip occurring in the stimulated zone (e.g., Cornet and Julie, 1989; Schoenball et al., 2014). Although these stress changes have been shown to be on the order of tens of MPa, they are generally confined to the region experiencing shear failure (Schoenball et al., 2014). It is therefore less obvious how large of an influence this stress redistribution may have outside of the previously stimulated zone. It is fairly difficult to account for this type of stress redistribution using current models. It may be the case that this effect is seen to play a significant role if this methodology is tested at the field scale.

For this analysis, an isothermal approach was taken. It is true that large temperature differences may exist between the stimulating fluid and the reservoir and other authors have suggested that thermal strains should be considered (e.g., Ghassemi and Tao, 2016). However, given the relatively small volumes of fluid injected during a stimulation treatment, thermal strains are only likely to have a moderate effect on the stress field. For example, considering that over the course of the stimulation 8778 kg/m of fluid was injected, a first order approximation of the thermal strain induced over a 300m radius from the wellbore can be calculated assuming that the injected fluid is 80 °C cooler than the reservoir. This radius results in a volume of investigation of 282743 m^3 per meter of wellbore. Then, by solving for T_B, the temperature at equilibrium, in the following enthalpy balance equation,

$$V(1-\varphi)\rho_s cp_s T_{res} + cp_f M_{inj} T_{inj} + cp_f\left(\varphi\rho_f V - M_{inj}\right)T_{res} = T_B V(1-\varphi)\rho_s cp_s + T_B V\varphi cp_f \rho_f \quad (7)$$

it can be seen that the temperature in this section reservoir, were it to be uniform, only decreases by 0.004 °C during stimulation. Next, this temperature decrease can be found to lead to a stress change of -0.0011 MPa based on,

$$\Delta S = \frac{1-2\nu}{1-\nu}\alpha_d \Delta T, \quad (8)$$

which employs an assumption of no horizontal strains (Cheng 2016), a simplification for a first order analysis. Note that all parameters used to make this calculation are shown in Table 1 along with their definitions. The Bulk modulus is found using the Poisson's ratio and Young's modulus used previously. The thermoelastic effective stress coefficient is the product of Bulk modulus and the volumetric expansion coefficient, which is based on Fjaer et al., 2008.

Table 1: Parameters used for the thermal stress calculation

Name	Variable	Value
Volume of investigation	V	$282743\ \frac{m^3}{m}$
Mass injected	M_{inj}	$8778\ \frac{kg}{m}$
In-situ temperature	T_{res}	$453\ K$
Fluid temperature	T_{inj}	$373\ K$
Porosity	ϕ	0.02
Heat capacity rock	cp_s	$950\ \frac{J}{kgK}$
Heat capacity fluid	cp_f	$4183\ \frac{J}{kgK}$
Density rock	ρ_s	$2700\ \frac{kg}{m^3}$
Density fluid	ρ_f	$1000\ \frac{kg}{m^3}$
Poisson's ratio	ν	0.15
Volumetric expansion coefficient	β_d	$4e^{-5}\ \frac{1}{K}$
Drained bulk modulus	K	$8.6\ GPa$
Thermoelastic effective stress coefficient	α_d	$0.344\ \frac{MPa}{K}$

Based on these calculations it is clear that thermal strains have a limited influence in this case. It is possible that the cooling would have significant local effects near the wellbore; however, this region is not the primary concern of this investigation.

5.2 Implications for EGS

The shear failure induced by the fluid production during phase 2 implies that the regular operation of a geothermal doublet system could lead to induced shear failure above the producing well. Although it is unclear in this analysis if this shear failure could be significant from an induced seismicity perspective, the production-induced seismicity seen in the oil and gas industry (Segall 1989) implies that, given the correct circumstances, it may be possible to induce small- to moderately-sized earthquakes in this way. It should be noted, however, that a geothermal doublet well typically operates with balanced fluid injection/production. Generally, operations which balance fluid volumes have a smaller chance of inducing significant levels of seismicity.

The ability to direct a shear stimulation treatment would afford reservoir engineers more possibilities in developing a geothermal reservoir. It may help in ensuring that fluids spend a sufficient amount of time in the reservoir while circulating, mitigating short circuiting. Further, it may be used to avoid stimulating a potentially seismic fault that is located reasonably close to a well. Of course, the ability to attract a stimulation treatment towards a well would also be useful and would help ensure inter-well connectivity. Although, in the example shown, the proposed methodology would not be able to attract a stimulation treatment towards another well, this may be possible in a normal faulting stress regime. In a normal faulting stress regime, the minimum principal stress is horizontal. As this methodology reduces the horizontal stresses between the two wells, it may be able to precondition the stress field such that stimulation treatments are attracted toward previously stimulated zones in normal faulting stress regimes. Strike-slip faulting stress regimes are less obvious to evaluate because both the minimum and maximum principal stresses are horizontal; however, the in plane and out of plane horizontal stresses do not change by equal amounts during production. Therefore, in a strike-slip faulting stress regime, it may be possible to design stimulation treatments that are either repelled or attracted to previously depleted zones depending on the well bores' orientations with respect to the prevailing stress field.

It has been suggested here that shear stimulation treatments can be repelled in critically-stressed reservoirs. In order to confirm these results, experimental work would have to be carried out in a rock laboratory. If those experiments were to prove to be successful, other methodologies could be developed, not only for other stress regimes, but also for less critically-stressed reservoirs.

6. CONCLUSION

It has been suggested that is possible to repel shear stimulation treatments in critically-stressed fractured granitic reservoirs using a stress preconditioning production phase in a previously stimulated section of the reservoir. This methodology has been shown for reverse faulting stress regimes. The poroelastic stress changes associated with production and not the pore pressure reductions are responsible for directing the shear stimulation treatment of a well in virgin rock away from the previously stimulated section of reservoir. These results have reservoir engineering implications for EGS reservoirs and may help to mitigate flow short circuiting and certain cases of potential induced seismicity. Variations of this methodology may be developed for other stress regimes and may also be able to attract, as opposed to strictly repel, stimulation treatments towards other wells.

7. ACKNOWLEDGEMENTS

This work has been supported by a research Grant (SI/500963-01) of the Swiss Federal Office of Energy. Xiaodong Ma received funding from the Swiss Competence Center for Energy Research – Supply of Electricity and Swiss National Science Foundation Grant No. 182150. No new data were used in producing this manuscript.

REFERENCES

Aziz, K., and Settari, A.: Petroleum Reservoir Simulation. Blitzprint Ltd., Calgary, Alberta (2002).

Baria, R., Michelet, S., Baumgaertner, J., Dyer, B., Gerard, A., Nicholls, J., Hettkamp, T., Teza, D., Soma, N., Asanuma, H., Garnish, J., and Megel, T.: Microseismic monitoring of the World's largest potential HDR Reservoir, In: *Twenty-Ninth Workshop on Geothermal Reservoir Engineering Stanford University, Stanford, California, January 26-28, 2004*, (2004).

Biot, M.: General theory of three-dimensional consolidation, *Journal of Applied Physics*, **12**, (1941), 155-164.

Boutéca, M., Lessi, J., and Sarda, J.: Stress changes induced by fluid injection in a porous layer around a wellbore, In: *24th U.S. Symposium on Rocks Mechanics June 1983*, (1983).

Brudy, M., Zoback, M., Fuchs, K., Rummel, F., and Baumgärtner, J.: Estimation of the complete stress tensor to 8 km depth in the KTB scientific drill holes: Implications for crustal strength, *Journal of Geophysical Research*, **102**, (1997), 18453-18475.

Catalli, F., Meier, M., and Wiemer, S.: The role of Coulomb stress changes for injection-induced seismicity: The Basel enhanced geothermal system, *Geophysical Research Letters*, **40**, (2013), 72-77.

Chen, X., Nakata, N., Pennington, C., Haffener, J., Chang, J., He, X., Zhan, Z., Ni, S., and Walter, J.: The Pawnee earthquake as a result of the interplay among injection, faults and foreshocks, *Scientific Reports*, **7**, (2017).

Cheng, A.: On generalized plane strain poroelasticity, *International Journal of Rock Mechanics and Mining Sciences*, **35**, (1998), 183-193.

Cheng, A.: Poroelasticity. Springer Nature (2016).

Cornet, F., and Julien, P.: Stress determination from hydraulic test data and focal mechanisms of induced seismicity, *International Journal of Rock Mechanics and Mining Sciences & Geomechanics Abstracts*, **26**, (1989), 235-248.

Deng, K., Liu, Y., and Harrington, R.: Poroelastic stress triggering of the December 2013 Crooked Lake, Alberta, induced seismicity sequence, *Geophysical Research Letters*, **43**, (2016), 8482-8491.

Evans, K., Dahlø, T., and Roti, J.: Mechanisms of pore pressure stress coupling which can adversely affect stress measurements conducted in deep tunnels, *Pure and Applied Geophysics*, **160**, (2003), 1087-1102.

Evans, K., Genter, A., and Sausse, J: Permeability creation and damage due to massive fluid injections into granite at 3.5 km at Soultz 1. Borehole observations, *Journal of Geophysical Research*, **110**, (2005a).

Evans, K., Moriya, H., Niitsuma, H., Jones, R., Phillips, W., Genter, A., Sausse, J., Jung, R., and Baria, R.: Microseismicity and permeability enhancement of hydrogeologic structures during massive fluid injections into granite at 3 km depth at the Soultz HDR site, *Geophysical Journal International*, **160**, (2005b), 388-412.

Evans, K., Zappone, A., Kraft, T., Deichmann, N., and Moia, F.: A survey of the induced seismic responses to fluid injection in geothermal and CO_2 reservoirs in Europe, *Geothermics*, **41**, (2012), 30-54.

Fjaer, E., Holt, R., Horsrud, P., Raaen, A., and Risnes, R.: Petroleum Related Rock Mechanics. Elsevier B.V., Amsterdam, The Netherlands (2008).

Ghassemi, A., and Tao, Q.: Thermo-poroelastic effects on reservoir seismicity and permeability change, *Geothermics*, **63**, (2016), 210-224.

Häring, M., Schanz, U., Ladner, F., and Dyer, B.: Characterisation of the Basel 1 enhanced geothermal system, *Geothermics*, **37**, (2008), 469-495.

Jupe, A., Green, A., and Wallroth, T.: Induced microseismicity and reservoir growth at the Fjällbacka Hot Dry Rocks Project, Sweden, *International Journal of Rock Mechanics and Mining Sciences & Geomechanics Abstracts*, **29**, (1992), 343-354.

Kwiatek, G., Saarno, T., Ader, T., Bluemle, F., Bohnhoff, M., Chendorain, M., Dresen, G., Heikkinen, P., Kukkonen, I., Leary, P., Leonhardt, M., Malin, P., Martinez-Garzon, P., Passmore, K., Passmore, P., Valenzuela, S., and Wollin, C.: Controlling fluid-induced seismicity during a 6.1-km-deep geothermal stimulation in Finland, *Science Advances*, **5**, (2019).

Ladner, F., and Häring, M.: Hydraulic characteristics of the Basel 1 Enhanced Geothermal System, *Geothermal Resources Council Transactions*, **33**, (2009), 199-204.

McClure, M., and Horne, R.: An investigation of stimulation mechanisms in Enhanced Geothermal Systems, *International Journal of Rock Mechanics & Mining Sciences*, **71**, (2014), 242-260.

Miller, S. A.: Modeling enhanced geothermal systems and the essential nature of large-scale changes in permeability at the onset of slip, *Geofluids*, **15**, (2015), 338-349.

Pearson, C.: The relationship between microseismicity and high pore pressures during hydraulic stimulation experiments in low permeability granitic rocks, *Journal of Geophysical Research*, **86**, (1981), 7855-7864,

Pimienta, L., Orellana, L. F., and Violay, M.: Variations in elastic and electrical properties of crustal rocks with varying degree of microfracturation, *Journal of Geophysical Research: Solid Earth*, **124**, (2019).

Rice, J., and Cleary, M.: Some basic stress diffusion solutions for fluid-saturated elastic porous media with compressible constituents, *Reviews of Geophysics and Space Physics*, **14**, (1976), 227-241.

Robinson, E., Potter, R., McInteer, B., Rowley, J., Armstrong, D., and Mills, R.: A preliminary study of the nuclear subterrene (LA-4547), (1971).

Schoenball, M., Dorbath, L., Gaucher, E., Wellmann, J., and Kohl, L.: Change of stress regime during geothermal reservoir stimulation, *Geophysical Research Letters*, **41**, (2014), 1163-1170.

Shuck, L.: Method for selectively orienting induced fractures in subterranean Earth formations, (1977), U.S. Patent No. 4005750.

Segall, P.: Earthquakes triggered by fluid extraction, *Geology*, **17**, (1989), 942-946.

Stein, R.: The role of stress transfer in earthquake occurrence, *Nature*, **402**, (1999), 605-609.

Villeneuve, M., Heap, M., Kushnir, A., Qin, T., Baud, P., Zhou, G., and Xu, T.: Estimating in situ rock mass strength and elastic modulus of granite from the Soultz-sous-forêts geothermal reservoir (France), *Geothermal Energy*, **6**, (2018).

Walsh, J.: The effect of cracks in rocks on poisson's ratio, *Journal of Geophysical Research*, **70**, (1965), 5249-5257.

Wang, H.: Theory of Linear Poroelasticity with Applications to Geomechanics and Hydrogeology. Princeton Series in Geophysics, Princeton University Press, Princeton, NJ (2000).

Warpinski, N., and Branagan, P.: Altered-stress fracturing, *Journal of Petroleum Technology*, **41**, (1989), 990-997.

Zang, A., Oye, V., Jousset, P., Deichmann, N., Gritto, R., McGarr, A., Majer, E., and Bruhn, D.: Analysis of induced seismicity in geothermal reservoirs – An overview, *Geothermics*, **52**, (2014), 6-21.

Ziagos, J., Phillips, B., Boyd, L., Jelacic, A., Stillman, G., and Hass, E.: A technology roadmap for strategic development of enhanced geothermal systems, *Proceedings,* Thirty-Eighth Workshop on Geothermal Reservoir Engineering, Stanford University, Stanford, CA (2013).

Zoback, M., and Townend, J.: Implications of hydrostatic pore pressures and high crustal strength for the deformation of intraplate lithosphere, *Tectonophysics*, **336**, (2001), 19-30.